Hindawi Publishing Corporation
International Journal of Photoenergy
Volume 2015, Article ID 841614, 8 pages
http://dx.doi.org/10.1155/2015/841614

Research Article

Enhancement of Spectral Response in μc-$Si_{1-x}Ge_x$:H Thin-Film Solar Cells with a-Si:H/μc-Si:H P-Type Window Layers

Yen-Tang Huang, Cheng-Hang Hsu, and Chuang-Chuang Tsai

Department of Photonics and Institute of Electro-Optical Engineering, National Chiao Tung University, Hsinchu 30010, Taiwan

Correspondence should be addressed to Yen-Tang Huang; yen.tang.huang@gmail.com

Received 28 July 2014; Accepted 3 November 2014

Academic Editor: Salvatore Lombardo

The hydrogenated amorphous silicon (a-Si:H)/hydrogenated microcrystalline silicon (μc-Si:H) double p-type window layer has been developed and applied for improving microcrystalline silicon-germanium p-i-n single-junction thin-film solar cells deposited on textured SnO_2:F-coated glass substrates. The substrates of SnO_2:F, SnO_2:F/μc-Si:H(p), and SnO_2:F/a-Si:H(p) were exposed to H_2 plasma to investigate the property change. Our results showed that capping a thin layer of a-Si:H(p) on SnO_2:F can minimize the Sn reduction during the deposition process which had H_2-containing plasma. Optical measurement has also revealed that a-Si:H(p) capped SnO_2:F glass had a higher optical transmittance. When the 20 nm μc-Si:H(p) layer was replaced by a 3 nm a-Si:H(p)/17 nm μc-Si:H(p) double window layer in the cell, the conversion efficiency (η) and the short-circuit current density (J_{SC}) were increased by 16.6% and 16.4%, respectively. Compared to the standard cell with the 20 nm μc-Si:H(p) window layer, an improved conversion efficiency of 6.19% can be obtained for the cell having a-Si:H(p)/μc-Si:H(p) window layer, with $V_{OC} = 490$ mV, $J_{SC} = 19.50$ mA/cm^2, and FF = 64.83%.

1. Introduction

Hydrogenated microcrystalline silicon (μc-Si:H) has attracted attentions as a promising material for an absorbing layer in Si-based thin-film solar cells [1–3]. Compared to hydrogenated amorphous silicon (a-Si:H), μc-Si:H has a higher resistance to Staebler-Wronski effect [4]. The effect generally found in amorphous materials could lead to the light-induced degradation [5–7] which deteriorates the long-term film quality as well as the efficiency in solar cells. Moreover, in contrast to the wider bandgap of 1.73 eV for a-Si:H [8], an extended near-infrared (NIR) response arising from the narrower bandgap of 1.1 eV [9, 10] of μc-Si:H film can be attained. However, μc-Si:H has a low absorption coefficient due to its indirect bandgap. A relatively thick μc-Si:H absorber is required for generating sufficient photon-excited carriers. For reducing the thickness of μc-Si:H absorber, μc-$Si_{1-x}Ge_x$:H has been employed as an absorber. Matsui et al. [11] reported that adding Ge into microcrystalline Si-Si network effectively enhanced NIR spectral response. For a μc-$Si_{1-x}Ge_x$:H film having Ge content of 50 at.%, approximately one order of absorption coefficient greater than that of μc-Si:H was observed. The absorption coefficient can achieve 10^4 cm^{-1} at 1.5 eV for μc-$Si_{1-x}Ge_x$:H. Matsui et al. [12] have later revealed that the μc-$Si_{1-x}Ge_x$:H single-junction solar cell achieved a cell efficiency of 6.3% with Ge content of approximately 20 at.% in the absorber.

For Si-based thin-film solar cells, the quality of the front transparent conducting oxide (TCO) also significantly influences the cell performance. The textured SnO_2:F-coated glass substrates have been widely applied. To promote the crystallization of μc-Si:H films, a highly H_2-containing gas mixture of H_2 and SiH_4 is generally utilized. Although there is a p-type layer on the TCO surface, the energetic hydrogen atom impinging on the surface can further penetrate inyo subsurface growth zone (up to 20 nm) [13–16]. When the SnO_2:F is directly or indirectly exposed to H_2-containing plasma, Sn reduction could appear and degrade cell performance due to the decreased light absorption [17–19]. In contrast to μc-Si:H film, we have found that adding GeH_4 for μc-$Si_{1-x}Ge_x$:H growth had an adverse effect on crystallization. A much higher H_2 dilution is required to maintain the crystallization of μc-$Si_{1-x}Ge_x$:H films. Thus, to alleviate unfavorable Sn reduction of SnO_2:F surface is one

Table 1: Parameters for different growth processes and H_2-plasma treatment.

Parameter	unit	a-Si:H(p)	μc-Si:H(p)	μc-$Si_{1-x}Ge_x$:H(i)	μc-SiO_x:H(n)	H_2 Plasma
Power density	mW/cm^2	34	325	148	44	325
Growth pressure	pa	40	500	1200	600	500
H_2 flow	sccm	50	800	1128–1960	1500	800
SiH_4 flow	sccm	20	10	15	11	0
GeH_4 flow	sccm	0	0	0.8	0	0
2% B_2H_6/H_2 flow	sccm	10	5	0	0	0
1% PH_3/H_2 flow	sccm	0	0	0	5	0
CO_2 flow	sccm	0	0	0	6	0

of the key issues for achieving high-efficiency μc-$Si_{1-x}Ge_x$:H cells.

Previous works [20, 21] have indicated that zinc oxide (ZnO) has a higher resistance to H_2-containing plasma environment. A thin aluminum-doped zinc oxide (AZO) layer deposited onto SnO_2:F surface has been proposed as a protection layer [22, 23]. However, a magnetron sputtering and a post-annealing treatment may generally be required for reducing the defects of the sputtered AZO and improving AZO/SnO_2:F interface. In this contribution, we introduced a simple in situ PECVD method to protect the SnO_2:F from Sn reduction. The double p-type window layer of a-Si:H/μc-Si:H has been developed to improve cell performance of μc-$Si_{1-x}Ge_x$:H p-i-n single-junction solar cells. We have investigated the effect of H_2 plasma on the transmittance and the surface morphology of the SnO_2:F. The results demonstrated that capping a thin p-type amorphous silicon (a-Si:H(p)) on SnO_2:F can minimize unfavorable Sn reduction during the deposition of microcrystalline films.

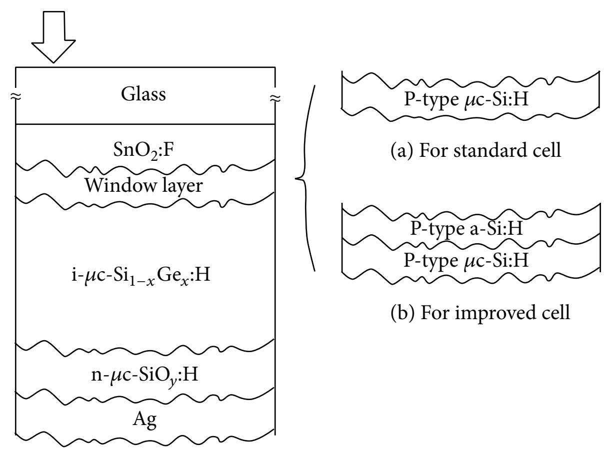

Figure 1: Schematic diagrams of the μc-$Si_{1-x}Ge_x$:H p-i-n single-junction solar cells with two types of the window layers: (a) 20 nm μc-Si:H(p) and (b) 3 nm a-Si:H(p)/17 nm μc-Si:H(p).

2. Experimental Details

In this work, Si-based films were deposited by a 27.12 MHz multichamber plasma-enhanced chemical vapor deposition (PECVD) system with a single chamber process at a substrate temperature of approximately 200°C. The parameters for different growth processes and H_2-plasma treatment were added in Table 1. The germane flow ratio and hydrogen ratio for SiGe alloys were defined as $R_{GeH4} = [GeH_4]/([GeH_4] + [SiH_4])$ and $R_{H2} = [H_2]/([GeH_4] + [SiH_4])$, respectively. The hydrogen ratio was varied from 71.4 to 124 with R_{GeH4} of 0 and 5.06%. The dark and the photoconductivities were measured by an I-V measurement system under dark and AM1.5G illumination. The standard cell structure was textured SnO_2:F-coated glass/μc-Si:H(p)/0.9 μm μc-$Si_{0.88}Ge_{0.12}$:H/μc-SiO_y:H(n)/Ag, as shown in Figure 1(a). In our previous work [24], the optimization and details of μc-$Si_{1-x}Ge_x$:H absorber were reported. The optimized μc-$Si_{1-x}Ge_x$:H absorber was deposited at R_{GeH4} = 5.06% and R_{H2} = 95.2, which corresponded to a Ge content of approximately 12 at.%. The film Ge content was evaluated by an X-ray photoelectron spectrometer. On the other hand, n-type μc-SiO_y:H was employed in the cells. N-type μc-SiO_y:H has been reported for improving cell performance in thin-film silicon solar cells [25, 26], in which there was less parasitic light loss in n-type layer and more long-wavelength reflection at i/n interface. Then, the cells were defined by the metal electrode with a cell area of 0.25 cm^2.

For standard cell, 20 nm thick μc-Si:H(p) layer was applied as a window layer. The μc-Si:H(p) layer was deposited by highly hydrogen-diluted SiH_4 and B_2H_6 ($[H_2]/[SiH_4] = 80$ and $[B_2H_6]/[SiH_4] = 1\%$) with 1-minute deposition time. The 200 nm thick μc-Si:H(p) layer has a conductivity of 6.82×10^{-1} S/cm. On the other hand, the 200 nm thick a-SiH(p) deposited with a relatively low H_2-to-SiH_4 ratio of 2.5 has a conductivity of 1.83×10^{-6} S/cm. The schematic structure of the improved cell is illustrated as Figure 1(b).

To investigate the change in the optical property, different film stacks on glass substrate including SnO_2:F, SnO_2:F/μc-Si:H(p) and SnO_2:F/a-Si:H(p) were prepared and exposed to the H_2 plasma for 1 minute. As can be seen in Table 1, the gas phase concentration of H_2 in the process of μc-Si:H(p) is 98.8% which is quite similar to the pure H_2 process (100%). Parameters such as pressure and power were kept the same for the H_2-plasma treatment and the deposition of μc-Si:H p-layer. This parameter setting should minimize the potential discrepancy between conditions treated by direct H_2-plasma exposure and the growth of μc-Si:H p-layer in the cell process. The samples were then measured by an ultraviolet-visible

Table 2: The optical transmittance (%) of the samples at the wavelength of 400 nm and 600 nm: glass/SnO_2:F, glass/SnO_2:F + H_2 plasma, glass/SnO_2:F/1–5 nm a-Si:H(p) + H_2 plasma, and glass/SnO_2:F/1–5 nm μc-Si:H(p) + H_2 plasma.

Wavelength (nm)	Raw SnO_2:F	SnO_2:F + H_2 plasma	SnO_2:F/a-Si:H(p) + H_2 plasma			SnO_2:F/μc-Si:H(p) + H_2 plasma		
			1 nm	3 nm	5 nm	1 nm	3 nm	5 nm
400	73.5	68.3	69.7	71.8	70.3	68.7	68.0	68.1
600	81.8	80.2	80.3	81.5	80.2	79.6	79.6	79.3

spectrophotometry for optical transmittance. The scanning electron microscope (SEM) was also used to reveal the surface morphologies. The experiments of optical transmittance and characterization of surface morphology changes provided clues for the TCO reduction. Furthermore, we characterized the cell performance by an *I-V* measurement system and a solar simulator under AM1.5G illumination. The quantum efficiency (QE) measurement was used to analyze the spectral response in the range of 300–1100 nm.

3. Results and Discussion

3.1. Effect of Hydrogen Ratio on Microcrystalline Si and SiGe Thin Films. Figure 2(a) shows the crystalline volume fraction (X_C) of μc-Si:H and μc-$Si_{1-x}Ge_x$:H films as a function of hydrogen ratio. When the hydrogen ratio was increased, an increase in the X_C was observed. With a higher hydrogen ratio in the plasma, more atomic hydrogen promotes the crystallization. In contrast to μc-Si:H film, a higher hydrogen dilution was needed to have the same X_C for μc-$Si_{1-x}Ge_x$:H. With an X_C of approximately 50%, the hydrogen ratios for μc-Si:H and μc-$Si_{1-x}Ge_x$:H growth were 80 and 95.2, respectively. The result suggested that the crystallization of the silicon film is suppressed by adding Ge. The difference in the atomic radius interrupts the ordered crystalline network which reduces the degree of crystallization. Moreover, the GeH_3 related species on the film surface during deposition were relatively harder to reach relaxation, which also decreases the crystalline volume fraction. In Figure 2(b), it can be seen that the photo- and dark conductivities of μc-Si:H and μc-$Si_{1-x}Ge_x$:H films increased with raising the hydrogen ratio. With a similar X_C of 50%, μc-Si:H and μc-$Si_{1-x}Ge_x$:H films had the dark conductivities of 7.63×10^{-8} and 6.62×10^{-7} S/cm, with the photoconductivities of 1.86×10^{-5} and 1.06×10^{-5} S/cm, respectively. Compared to μc-Si:H, the lower photoconductivity and the higher dark conductivity of μc-$Si_{1-x}Ge_x$:H were obtained. The more defective μc-$Si_{1-x}Ge_x$:H films were mainly due to the Ge incorporation which induces Ge-related defects in the films [11, 12].

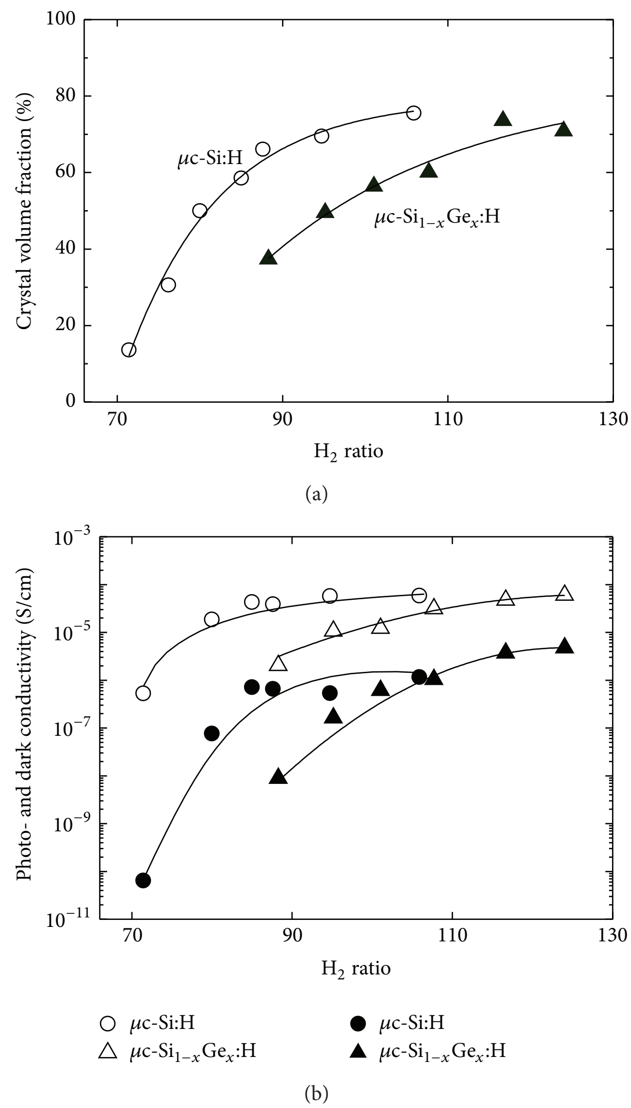

Figure 2: (a) Crystalline volume fraction and (b) conductivity as a function of hydrogen ratio for μc-Si:H (R_{GeH4} = 0) and μc-$Si_{1-x}Ge_x$:H (R_{GeH4} = 5%). In (b), the open and closed symbols represent the photo- and the dark conductivities, respectively.

3.2. Effect of H_2 Plasma on SnO_2:F-Coated Glass Substrate. As discussed in the previous section, silicon film with Ge incorporation requires a relatively higher hydrogen ratio to have appropriate crystallization. To suppress the Sn reduction of SnO_2:F due to hydrogen plasma during the deposition of the window layer is beneficial for the development of p-i-n μc-$Si_{1-x}Ge_x$:H single-junction solar cells.

Table 2 shows the optical transmittance of the different film-stacked glass substrates with or without the H_2-plasma treatment. In order to quantify the difference, the transmittance at the wavelength of 400 nm and 600 nm was compared. When the textured SnO_2:F-coated glass was treated by the H_2-plasma treatment for 1 minute, the transmittance decreased by 2.9% and 1.6% at 400 nm and 600 nm, respectively, compared to the fresh SnO_2:F-coated glass. This transmittance loss of SnO_2:F after H_2-plasma treatment has

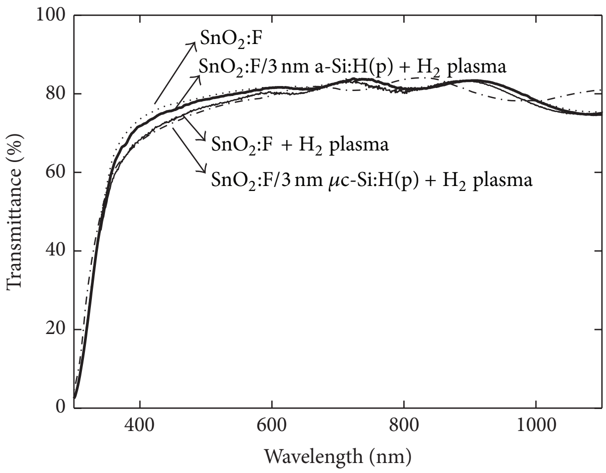

FIGURE 3: The optical transmittance of glass/SnO_2:F (dot line), glass/SnO_2:F + H_2 plasma (slim line), glass/SnO_2:F/3 nm a-Si:H(p) + H_2 plasma (bold line), and glass/SnO_2:F/3 nm μc-Si:H(p) + H_2 plasma (dash line).

also been demonstrated by Wallinga et al. [18]. For the SnO_2:F underwent H_2-plasma treatment, the binding energies of Sn in $3d_{5/2}$ orbit shifted to 486.5 eV and 484.8 eV, related to suboxides of tin and metallic tin [18, 19]. Therefore, the suboxides and the metallic Sn reduce the transmittance.

Compared to μc-Si:H(p), a much lower H_2-to-SiH_4 ratio was used for the deposition of a-Si:H(p) layer. As shown in Table 2, after being treated by H_2 plasma for 1 minute, the sample having structure of SnO_2:F/a-Si:H(p) had higher transmittance, compared to the raw SnO_2:F substrate. When the thickness of a-Si:H(p) on SnO_2:F increased from 1 nm to 3 nm, the transmittance at 400 nm increased from 69.7% to 71.8% and the transmittance at 600 nm increased from 80.3% to 81.5%. On the contrary, the transmittance decreased to 70.3% and 80.2% at 400 nm and 600 nm, respectively, as the thickness of a-Si:H(p) increased to 5 nm. Considering the trade-off between SnO_2:F protection and optical transmission, a 3 nm thick a-Si:H(p) layer was suited for SnO_2:F substrate. Moreover, the H_2-plasma treated SnO_2:F/μc-Si:H(p) had the worst transmittance, compared to the H_2-plasma treated SnO_2:F-coated glass and the H_2-plasma treated SnO_2:F/a-Si:H(p). This should be due to the higher hydrogen dilution during the deposition of μc-Si:H(p) and the less dense μc-Si:H film for resisting hydrogen penetration.

Figure 3 shows the optical transmittance of different glass substrates in the wavelength ranged from 300 to 1100 nm. The results show that the transmittance of the H_2-plasma treated SnO_2:F/3 nm a-Si:H(p) glass substrate was greater than that of the H_2-plasma treated SnO_2:F glass substrate. For the wavelength shorter than 780 nm, the H_2-plasma treated SnO_2:F/3 nm a-Si:H(p) glass substrate exhibited a superior transmittance, compared to the H_2-plasma treated SnO_2:F/3 nm μc-Si:H(p) glass substrate. Depositing a thin layer of a-Si:H(p) could be suitable for a microcrystalline silicon process on SnO_2:F based glass substrates.

Figures 4(a), 4(c), and 4(e) show the SEM images of the SnO_2:F surface, SnO_2:F surface covered with 3 nm thick a-Si:H(p), and SnO_2:F surface covered with 3 nm thick μc-Si:H(p) before the hydrogen plasma treatment, respectively. The surface morphologies of SnO_2:F surface covered with 3 nm thick films (Figures 4(c) and 4(e)) were both similar to the surface morphology of SnO_2:F before hydrogen plasma treatment (Figure 4(a)). To emulate the morphological change after the growth of p-type window layer in the cell process, the samples were treated with 1-minute H_2 plasma. As can be seen in Figure 4(b), the surface of the H_2-plasma treated SnO_2:F had many small particle-like structures with a size of approximately 20 nm, which indicated that the H_2 plasma significantly changed the surface morphology. Study had reported that it could be due to the Sn reduction or surface damage by H_2 plasma [27]. When the SnO_2:F is capped with a 3 nm thick a-Si:H(p) layer followed by the H_2-plasma treatment, the nanostructures were effectively decreased, as shown in Figure 4(d). In contrast, Figure 4(f) showed that the H_2 plasma still significantly changed the surface morphology of the SnO_2:F which was capped with a 3 nm thick μc-Si:H(p) layer. This surface morphology was similar to the surface of the H_2-plasma treated SnO_2:F. According to these results, a 3 nm thick a-Si:H(p) layer can minimize the effect of H_2 plasma on the SnO_2:F surface, while maintaining acceptable optical performance. Regarding the surface coverage of the 3-nm thick films on the textured SnO_2:F surface, Tsai et al. have reported that the device-quality a-Si:H films were deposited conformally on the substrates with aspect ratio (width/height) ranging from 0.2 to 2 [28]. Since the random pyramidal-like texture of SnO_2:F-coated substrates had smoother surface with roughness of approximately 40 nm and correlation length of approximately 175 nm [29, 30], a 3 nm thick a-Si:H(p) or a 3 nm thick μc-Si:H(p) film can effectively cover the SnO_2:F surface.

3.3. Improving the Cell Performance of μc-SiGe:H Single-Junction Cells by Capping an a-Si:H(p) Film on SnO_2:F. Figures 5 and 6 show the J-V characteristics and the spectral responses, respectively, of the μc-$Si_{0.88}Ge_{0.12}$:H p-i-n solar cells with a 0.9 μm active layer. The cell performance of the μc-$Si_{0.88}Ge_{0.12}$:H p-i-n single-junction solar cells with different p-type window layer is demonstrated in Table 3. The thickness of p-type window layer was kept at 20 nm for comparison. The standard cell with a 20 nm thick single p-type μc-Si:H window layer can achieve a conversion efficiency of 5.31%. Based on the structure, we employed a 3 nm a-Si:H(p)/17 nm μc-Si:H(p) double window layer in the μc-$Si_{1-x}Ge_x$:H p-i-n single-junction solar cell. This cell with the double p-type window layer has an improved cell performance, especially in the short-circuit current (J_{SC}). Compared to the standard cell, the J_{SC} can be significantly enhanced from 16.75 to 19.50 mA/cm^2, which was a 16.4% improvement.

As can be seen in Figure 6, the cell with the a-Si:H(p)/μc-Si:H(p) double window layer had a greater quantum efficiency in the wavelength ranging from 300 to 1100 nm. It is also shown in Table 4 that the spectral response of the short wavelength (400 nm) was increased by 19.6% as compared

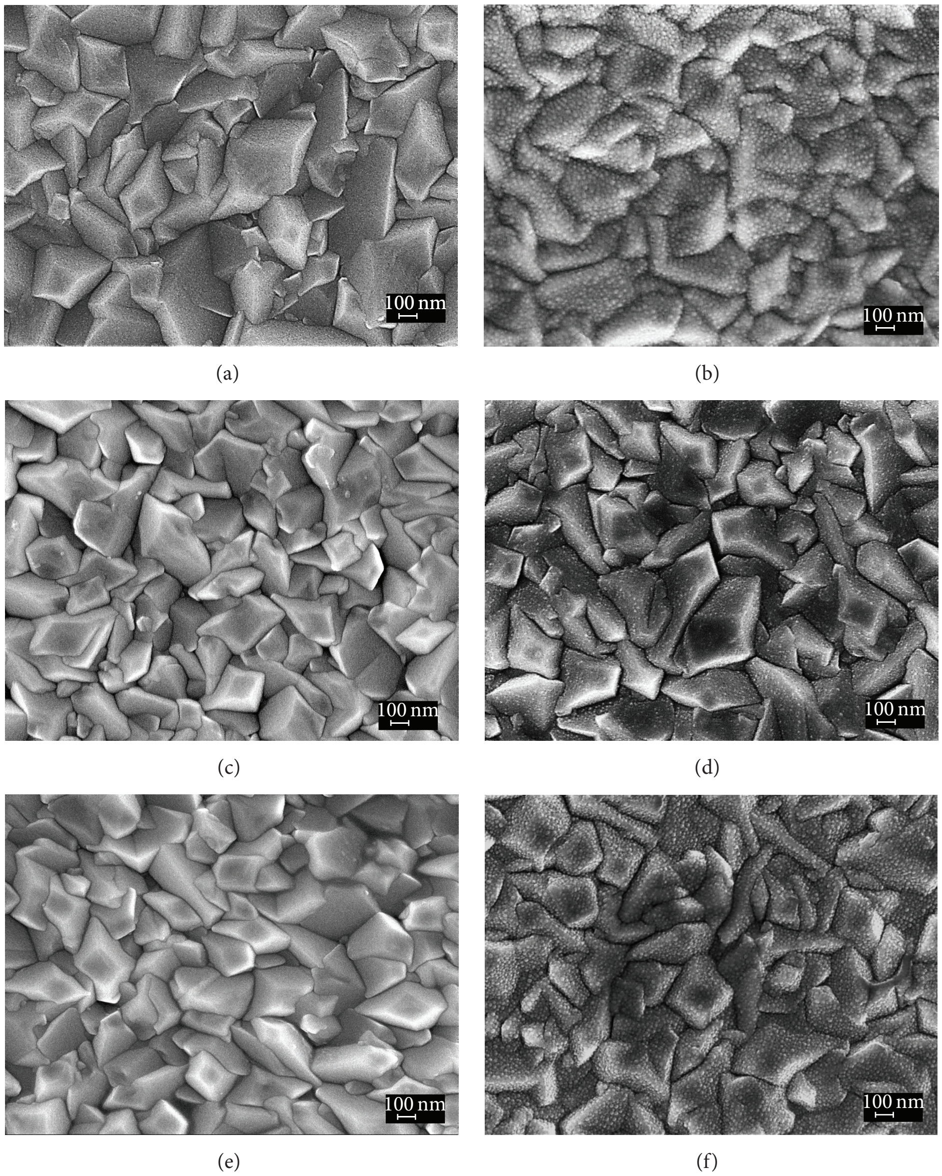

Figure 4: The scanning electron microscope (SEM) images of substrates having structures of (a) glass/SnO_2:F, (b) glass/SnO_2:F + H_2 plasma, (c) glass/SnO_2:F/3 nm a-Si:H(p), (d) glass/SnO_2:F/3 nm a-Si:H(p) + H_2 plasma, (e) glass/SnO_2:F/3 nm μc-Si:H(p), and (f) glass/SnO_2:F/3 nm μc-Si:H(p) + H_2 plasma.

Table 3: The cell performance of the μc-$Si_{0.88}Ge_{0.12}$:H p-i-n single-junction solar cells with different p-type window layers.

Window layer	V_{OC} (mV)	J_{SC} (mA/cm^2)	FF (%)	Eff. (%)
μc-Si:H(p)	480	16.75	66.08	5.31
a-Si:H(p)/μc-Si:H(p)	490	19.50	64.83	6.19
a-Si:H(p)/H_2 plasma/μc-Si:H(p)	500	18.19	64.77	5.89
H_2 plasma/a-Si:H(p)/μc-Si:H(p)	465	14.22	63.35	4.20

to the cell having only μc-Si:H(p). Moreover, the long-wavelength (800 nm) absorption was increased by 32.4%. The improved spectral response can be due to the less Sn reduction of the SnO_2:F surface. More incident light can get into the active layer of the cell and be absorbed to generate photoexcited carriers. Besides, the open circuit voltage (V_{OC}) was also enhanced by 10 mV. The larger V_{OC} could be attributed to a lower defect density at the TCO/p interface or in the p-layer, which has less metastable suboxides of tin and metallic tin arising from Sn reduction. The Sn reduction could also decrease work function of SnO_2:F which would lead to a larger potential barrier at the TCO/p interface.

Table 4: The external quantum efficiency at the wavelength of 400, 600, and 800 nm for the μc-$Si_{0.88}Ge_{0.12}$:H p-i-n single-junction solar cells with different p-type window layer.

Window layer	$QE_{400\,nm}$	$QE_{600\,nm}$ %	$QE_{800\,nm}$	J_{SC} (QE) mA/cm^2
μc-Si:H(p)	34.02	72.48	31.39	16.74
a-Si:H(p)/μc-Si:H(p)	40.68	79.58	41.56	19.25
a-Si:H(p)/H_2 plasma/μc-Si:H(p)	39.85	78.00	32.50	17.98
H_2 plasma/a-Si:H(p)/μc-Si:H(p)	22.45	65.31	26.94	14.47

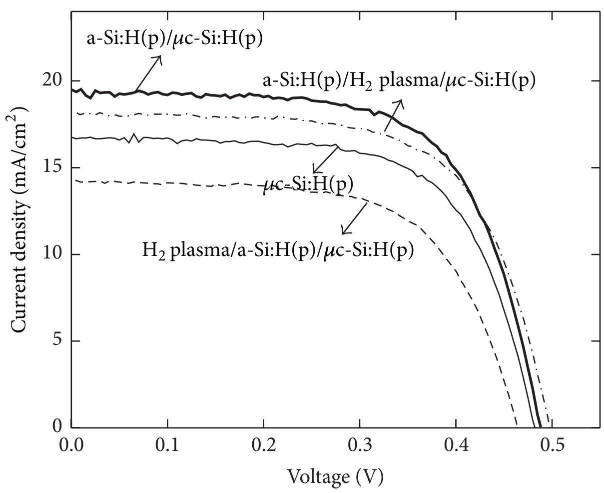

Figure 5: The J-V characteristics of μc-$Si_{0.88}Ge_{0.12}$:H p-i-n single-junction solar cells with different p-type window layers.

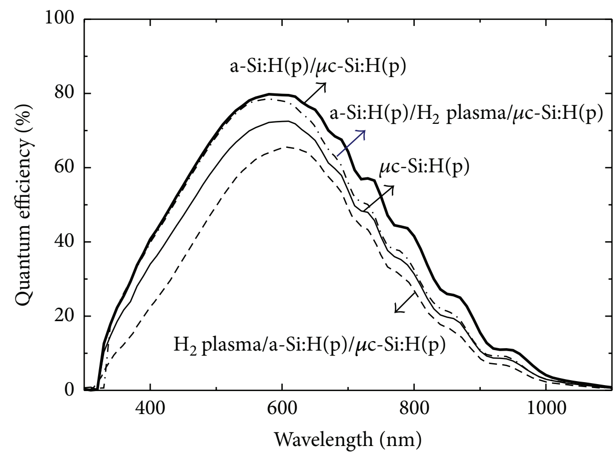

Figure 6: The quantum efficiency of μc-$Si_{0.88}Ge_{0.12}$:H p-i-n single-junction solar cells with different p-type window layers.

The SnO_2:F can be protected by capping the 3 nm thick a-Si:H(p) layer to minimize the Sn reduction which comes from the sequent films growth of μc-Si:H(p) and μc-$Si_{0.88}Ge_{0.12}$:H layers with high H_2-containing plasma environment. The improved TCO/p interface enhanced the built-in field and facilitated the carrier transport. As a result, the cell with the a-Si:H(p)/μc-Si:H(p) double window layer reached a greater conversion efficiency of 6.19%, which is significantly increased by 16.6% compared to the standard cell structure.

We have further investigated the durability of the double p-type window layer against Sn reduction of the SnO_2:F surface. When the H_2 plasma/a-Si:H(p)/μc-Si:H(p) structure was implemented as the window layer in the cell, the V_{OC} decreased to 465 mV and the J_{SC} decreased to 14.22 mA/cm^2. The drop of V_{OC} may be due to more defects at TCO/p interface. The significant absorption loss in the wavelength ranging from 300 to 1100 nm was revealed by the quantum efficiency measurement, which would lead to the decrease in J_{SC}. When the p-i-n cell was prepared on the direct H_2-plasma treated SnO_2:F surface, the reduction of SnO_2 liberated Sn, which could migrate into p-layer [31]. In addition, oxygen could also diffuse to p-layer and form SiO_x [31–34]. As a result, these defects led to a built-in potential loss which degraded cell performance of the device. On the other hand, using the a-Si:H(p)/H_2 plasma/μc-Si:H(p) structure as the window layer in the cell had only slight degradation of J_{SC} and V_{OC}, as compared to the optimized a-Si:H(p)/μc-Si:H(p) structure. This suggested that the 3 nm thick a-Si:H(p) layer reduced the effect of H_2 plasma on SnO_2:F surface compared to the H_2 plasma/a-Si:H(p)/μc-Si:H(p) structure. In contrast to the optimized cell, lower cell efficiency of 5.89% and J_{SC} of 18.19 mA/cm^2 were shown. The result indicates that the thin a-Si:H(p) layer cannot completely eliminate the effect of H_2 plasma on SnO_2:F surface. Certain amount of hydrogen radical could still affect SnO_2:F surface during the growth of a-Si:H(p) layer. However, considering the absorption loss arising from the a-Si:H(p) layer, a thickness of 3 nm is suited for optimizing the μc-SiGe:H single-junction cell performance.

On the other hand, the enhancement in EQE between cells with μc-Si:H(p) and a-Si:H(p)/μc-Si:H(p) can only be partly explained by the difference in transmittance observed between the H_2-plasma treated SnO_2:F and the 3 nm thick a-Si:H(p) capped SnO_2:F as shown in Figure 3. This indicated that the H_2 plasma also degraded the electrical property of the SnO_2:F substrates. Kambe et al. reported that [35] H_2-plasma treated SnO_2:F had an increased resistivity and a decreased hall mobility. In addition, the liberated Sn may migrate into the p-layer [31], which causes the degradation of the doped layer. In this study, the significant improvement of the cell performance should majorly arise from the improved TCO/p interface, accompanied with minor optical improvement. In comparison with the state-of-art μc-$Si_{1-x}Ge_x$:H cell with an efficiency of 8.2% (J_{SC} = 25.5 mA/cm^2, V_{OC} = 0.494 V, and

FF = 0.651) reported by Matsui et al. [36], the reference cell reported in this work exhibited comparable V_{OC} and FF but lower J_{SC}. The reduction in J_{SC} can be mainly attributed to the difference in front TCO layer and antireflection coating. The commercial SnO_2:F-coated substrate is much more chemically unstable in the hydrogen-rich plasma than the ZnO:Ga, which limited the J_{SC} of the reference cell. Furthermore, since the surface texture of commercial SnO_2:F-coated substrate is not optimized for the μc-$Si_{1-x}Ge_x$:H cell [36], the chemically etched ZnO:Ga should lead to an enhancement in J_{SC}. In our case, the lack of antireflection bilayer in the reference cell also posted a constraint on J_{SC} in our case [37]. We have demonstrated that the protection of SnO_2:F surface from the hydrogen-rich plasma significantly enhanced the J_{SC} from 16.75 to 19.50 mA/cm^2 in this work. Further improvement on performance of solar cell is expected as light-trapping technique and optimization on the process condition are performed in the current cell.

4. Conclusions

In conclusion, we have shown that H_2 plasma significantly degraded the transmittance and changed the surface morphology of SnO_2:F. An adequate thickness of a-Si:H(p) layer has been successfully applied to minimize the harmful H_2-plasma effect on SnO_2:F surface during the sequent deposition of μc-Si:H(p) and μc-SiGe:H layers. In contrast to the standard μc-$Si_{0.88}Ge_{0.12}$:H p-i-n single-junction cell with a 20 nm thick μc-Si:H(p) window layer, an improved cell performance can be achieved by employing the 3 nm a-Si:H(p)/17 nm μc-Si:H(p) window layer. Due to an improvement in TCO/p interface, the better spectral response at the wavelength of 300–1100 nm was observed. The corresponding J_{SC} increased from 16.75 to 19.50 mA/cm^2. As a result, the conversion efficiency was improved from 5.31% to 6.19% which was a marked increase of 16.6%.

Conflict of Interests

The authors do not have any conflict of interests with the content of the paper.

Acknowledgments

This study was sponsored by the National Science Council in Taiwan under contract nos. MOST-103-3113-P-008-001 and MOST-103-2221-E-009-068. The Instrument Center of the National Science Council has provided support to complete this research.

References

[1] A. V. Shah, J. Meier, E. Vallat-Sauvain et al., “Material and solar cell research in microcrystalline silicon,” *Solar Energy Materials and Solar Cells*, vol. 78, no. 1–4, pp. 469–491, 2003.

[2] K. Saito, M. Sano, S. Okabe, S. Sugiyama, and K. Ogawa, “Microcrystalline silicon solar cells fabricated by VHF plasma CVD method,” *Solar Energy Materials & Solar Cells*, vol. 86, no. 4, pp. 565–575, 2005.

[3] B. Yan, G. Yue, X. Xu, J. Yang, and S. Guha, “High efficiency amorphous and nanocrystalline silicon solar cells,” *Physica Status Solidi (A) Applications and Materials Science*, vol. 207, no. 3, pp. 671–677, 2010.

[4] D. L. Staebler and C. R. Wronski, “Reversible conductivity changes in discharge-produced amorphous Si,” *Applied Physics Letters*, vol. 31, no. 4, pp. 292–294, 1977.

[5] F. Meillaud, E. Vallat-Sauvain, X. Niquille et al., “Light-induced degradation of thin film amorphous and microcrystalline silicon solar cells,” in *Proceedings of the 31st IEEE Photovoltaic Specialists Conference*, pp. 1412–1415, January 2005.

[6] J. Meier, R. Flückiger, H. Keppner, and A. Shah, “Complete microcrystalline p-i-n solar cell—crystalline or amorphous cell behavior,” *Applied Physics Letters*, vol. 65, no. 7, pp. 860–862, 1994.

[7] M. Stutzmann, W. B. Jackson, and C. C. Tsai, “Light-induced metastable defects in hydrogenated amorphous silicon: a systematic study,” *Physical Review B*, vol. 32, no. 1, pp. 23–47, 1985.

[8] C. R. Wronski, S. Lee, M. Hicks, and S. Kumar, “Internal photoemission of holes and the mobility gap of hydrogenated amorphous silicon,” *Physical Review Letters*, vol. 63, no. 13, pp. 1420–1423, 1989.

[9] N. Beck, P. Torres, J. Fric et al., “Optical and electrical properties of undoped microcrystalline silicon deposited by the VHF-GD with different dilutions of silane in hydrogen,” *Proceedings of the Materials Research Society Symposium*, vol. 452, pp. 761–766, 1997.

[10] M. A. Green, “Third generation photovoltaics: solar cells for 2020 and beyond,” *Physica E: Low-Dimensional Systems and Nanostructures*, vol. 14, no. 1-2, pp. 65–70, 2002.

[11] T. Matsui, M. Kondo, K. Ogata, T. Ozawa, and M. Isomura, “Influence of alloy composition on carrier transport and solar cell properties of hydrogenated microcrystalline silicon-germanium thin films,” *Applied Physics Letters*, vol. 89, no. 14, Article ID 142115, 2006.

[12] T. Matsui, C.-W. Chang, T. Takada, M. Isomura, H. Fujiwara, and M. Kondo, “Microcrystalline Si1-xGex solar cells exhibiting enhanced infrared response with reduced absorber thickness,” *Applied Physics Express*, vol. 1, no. 3, Article ID 031501, 2008.

[13] K. Nakamura, K. Yoshino, S. Takeoka, and I. Shimizu, “Roles of atomic hydrogen in chemical annealing,” *Japanese Journal of Applied Physics*, vol. 34, no. 2, pp. 442–449, 1995.

[14] I. An, Y. Li, C. R. Wronski, and R. W. Collins, “Sub-surface equilibration of hydrogen with the a-Si:H network under film growth conditions,” *Materials Research Society Symposium Proceedings*, vol. 297, p. 43, 1993.

[15] A. Matsuda, “Growth mechanism of microcrystalline silicon obtained from reactive plasmas,” *Thin Solid Films*, vol. 337, no. 1-2, pp. 1–6, 1999.

[16] A. Matsuda, “Microcrystalline silicon.: growth and device application,” *Journal of Non-Crystalline Solids*, vol. 338–340, no. 1, pp. 1–12, 2004.

[17] R. Das, T. Jana, and S. Ray, “Degradation studies of transparent conducting oxide: a substrate for microcrystalline silicon thin film solar cells,” *Solar Energy Materials and Solar Cells*, vol. 86, no. 2, pp. 207–216, 2005.

[18] J. Wallinga, W. M. Arnoldbik, A. M. Vredenberg, R. E. I. Schropp, and W. F. van der Weg, “Reduction of tin oxide by hydrogen radicals,” *Journal of Physical Chemistry B*, vol. 102, no. 32, pp. 6219–6224, 1998.

[19] S. Major, M. C. Bhatnagar, S. Kumar, and K. L. Chopra, "The degradation of fluorine doped tin oxide films in a hydrogen plasma," *Journal of Vacuum Science and Technology A*, vol. 6, no. 4, pp. 2415–2420, 1988.

[20] S. Major, S. Kumar, M. Bhatnagar, and K. L. Chopra, "Effect of hydrogen plasma treatment on transparent conducting oxides," *Applied Physics Letters*, vol. 49, no. 7, pp. 394–396, 1986.

[21] S. Kumar and B. Drevillon, "A real time ellipsometry study of the growth of amorphous silicon on transparent conducting oxides," *Journal of Applied Physics*, vol. 65, no. 8, pp. 3023–3034, 1989.

[22] R. H. Franken, C. H. M. van der Werf, J. Löffler, J. K. Rath, and R. E. I. Schropp, "Beneficial effects of sputtered ZnO:Al protection layer on SnO_2:F for high-deposition rate hot-wire CVD p-i-n solar cells," *Thin Solid Films*, vol. 501, no. 1-2, pp. 47–50, 2006.

[23] A. Masuda, K. Imamori, and H. Matsumura, "Influence of atomic hydrogen on transparent conducting oxides during hydrogenated amorphous and microcrystalline Si preparation by catalytic chemical vapor deposition," *Thin Solid Films*, vol. 411, no. 1, pp. 166–170, 2002.

[24] Y. T. Huang, H. J. Hsu, S. W. Liang, C. H. Hsu, and C. C. Tsai, "Development of hydrogenated microcrystalline silicon-germanium alloys for improving long-wavelength absorption in Si-based thin-film solar cells," *International Journal of Photoenergy*, Article ID 579176, pp. 1–7, 2014.

[25] P. Delli Veneri, L. V. Mercaldo, and I. Usatii, "Silicon oxide based n-doped layer for improved performance of thin film silicon solar cells," *Applied Physics Letters*, vol. 97, no. 2, Article ID 023512, 2010.

[26] S. W. Liang, Y. T. Huang, H. J. Hsu, C. H. Hsu, and C. C. Tsai, "Applications of μc-SiO_x:H as integrated n-layer and back transparent conductive oxide for a-Si:H/μc-Si:H tandem cells," *Japanese Journal of Applied Physics*, vol. 53, no. 5S1, Article ID 05FV08, 2014.

[27] H. C. Weller, R. H. Mauch, and G. H. Bauer, "Novel type of ZnO studied in combination with 1.5eV a-SiGe:H pin diodes," in *Proceedings of the 22th IEEE Photovoltaic Specialists Conference*, pp. 1290–1295, Las Vegas, Nev, USA, October 1991.

[28] C. C. Tsai, J. C. Knights, G. Chang, and B. Wacker, "Film formation mechanisms in the plasma deposition of hydrogenated amorphous silicon," *Journal of Applied Physics*, vol. 59, no. 8, pp. 2998–3001, 1986.

[29] K. Jäger, M. Fischer, R. A. C. M. M. Van Swaaij, and M. Zeman, "A scattering model for nano-textured interfaces and its application in opto-electrical simulations of thin-film silicon solar cells," *Journal of Applied Physics*, vol. 111, no. 8, Article ID 083108, 2012.

[30] K. Sato, Y. Gotoh, Y. Wakayama, Y. Hayashi, K. Adachi, and H. Nishimura, "Highly textured Sn02:F TCO films for a-Si solar cells," *Reports of the Research Laboratory, Asahi Glass*, vol. 42, pp. 129–137, 1992.

[31] A. Nuruddin and J. R. Abelson, "Improved transparent conductive oxide/p^+/i junction in amorphous silicon solar cells by tailored hydrogen flux during growth," *Thin Solid Films*, vol. 394, no. 1-2, pp. 49–63, 2001.

[32] K. Kawabata, Y. Shiratsuki, T. Hayashi, K. Yamada, S. Miyazaki, and M. Hirose, "Diffusion barrier effect of ultra-thin photo-nitrided a-Si:H overlayer on SnO_2/glass substrate," *Japanese Journal of Applied Physics, Part 2: Letters*, vol. 30, no. 7B, pp. L1231–L1234, 1991.

[33] W. Beyer, J. Hüpkes, and H. Stiebig, "Transparent conducting oxide films for thin film silicon photovoltaics," *Thin Solid Films*, vol. 516, no. 2–4, pp. 147–154, 2007.

[34] A. Eicke and G. Bilger, "XPS and SIMS characterization of metal oxide/amorphous silicon-carbon interfaces," *Surface and Interface Analysis*, vol. 12, no. 6, pp. 344–350, 1988.

[35] M. Kambe, K. Sato, D. Kobayashi et al., "TiO_2-coated transparent conductive oxide (SnO_2:F) films prepared by atmospheric pressure chemical vapor deposition with high durability against atomic hydrogen," *Japanese Journal of Applied Physics*, vol. 45, no. 8–11, pp. L291–L293, 2006.

[36] T. Matsui, H. Jia, and M. Kondo, "Thin film solar cells incorporating microcrystalline $Si_{1-x}Ge_x$ as efficient infrared absorber: an application to double junction tandem solar cells," *Progress in Photovoltaics: Research and Applications*, vol. 18, no. 1, pp. 48–53, 2010.

[37] T. Fujibayashi, T. Matsui, and M. Kondo, "Improvement in quantum efficiency of thin film Si solar cells due to the suppression of optical reflectance at transparent conducting oxide/Si interface by TiO_2/ZnO antireflection coating," *Applied Physics Letters*, vol. 88, no. 18, Article ID 183508, 2006.